Fuel xxx (xxxx) xxx-xxx

Contents lists available at ScienceDirect

Fuel

journal homepage: http://ees.elsevier.com

Full Length Article

Experimental and numerical investigation of the Advanced Fuel Ignition Delay Analyzer (AFIDA) constant-volume combustion chamber as a research platform for fuel chemical kinetic mechanism validation

Jon Luecke [1,*], Mohammad J. Rahimi [1], Bradley T. Zigler, Ray W. Grout

National Renewable Energy Laboratory, 15013 Denver West Parkway, Golden, CO 80401, United States

ARTICLE INFO

Keywords
Constant volume combustion chamber
Fuel
CFD
Ignition delay
Chemical kinetic mechanism
AFIDA

ABSTRACT

Advanced combustion engine strategies that can offer increased efficiency and reduced emissions are enabled by numerical engine combustion simulations, requiring accurate chemical kinetic mechanism input. The Advanced Fuel Ignition Delay Analyzer (AFIDA) device can perform high quality, repeatable measurements of ignition delay (ID) times using small fuel quantities with high throughput. The AFIDA experiments involve liquid fuel injection into the heated and pressurized constant-volume chamber, producing an autoignition delay resulting from a combination of physical mixing and chemical kinetic processes, a complexity which makes the development of complementary numerical models necessary for the development and validation of chemical kinetic mechanisms. Modeling the device based on a homogenous approximation with reduced primary reference fuel (PRF) mechanism shows up to 75% error in the modeled vs. observed autoignition delay data for n-heptane and iso-octane at 10 bar (ϕ = 1.2–0.8) and 20 bar (ϕ = 0.6–0.4) over 973–648 K, whereas the use of a computational fluid dynamics (CFD) model reduces the discrepancy to within 25%. The homogenous approximation error is greatest for conditions where the observed ignition delay is short and the system is not sufficiently mixed (<30 ms), providing guidance to select a homogenous reactor vs. CFD modeling approach based upon desired accuracy. Experimental 20 bar iso-octane ID results show a larger magnitude of negative temperature coefficient chemistry compared to numerical results, indicating possible deficiencies in the PRF chemical kinetic mechanism. This characterization demonstrates the AFIDA as a capable research platform for chemical kinetic model development and validation.

1. Introduction

While diesel fuel combustion quality characterization is common practice using constant-volume combustion chambers (CVCCs), gasoline-range fuel testing methodology is a relatively new research area for these types of devices [1,2], and is often based on correlations with a derived cetane number. Nonetheless, the value of this approach has been shown for screening candidate fuels [3]. The use of CVCCs to generate derived or indicated cetane numbers for diesel fuels is generally preferred to conventional cetane engine testing due to the advantages of quick analysis time, much smaller fuel volume requirements, and better precision over traditional cooperative fuels research engine-based testing methodology [4–6], although the ASTM D613 method remains the referee testing procedure mainly due to legacy [7,8].

The Advanced Fuel Ignition Delay Analyzer (AFIDA) is the latest in a series of CVCCs designed to measure the ignition delay of diesel fuels and produce a cetane correlation from the result [5]. Previous CVCCs reasonably have fuel injection systems designed around their intended purpose of injecting diesel fuels, and do not provide enough line pressure or cooling to fully address boiling challenges presented from volatile fuels [9–11]. The AFIDA has considerable advantages over other CVCCs, including automation, its similarity to modern injection technologies used in vehicles today, and compatibility for volatile fuels with gasoline-like boiling ranges [12]. The AFIDA design, which in-

Abbreviations: 0D, zero-dimensional; 3D, three-dimensional; AFIDA, Advanced Fuel Ignition Delay Analyzer; CFD, computational fluid dynamics; CPC, constant pressure control; Co-Optima, Co-Optimization of Fuels & Engines; CVCC, constant-volume combustion chamber; FT, flow transducer; HTHR, high-temperature heat release; HPLC, high-pressure liquid chromatography; ID, ignition delay; IQT, Ignition Quality Tester; LTHR, low-temperature heat release; M, motor; MFC, mass flow controller; NIST, National Institute of Standards and Technology; NREL, National Renewable Energy Laboratory; NTC, negative temperature coefficient; ppmv, parts per million by volume; PRF, primary reference fuel; PT, pressure transducer; RBOB, renewable blendstock for oxygentate blending; S, solenoid valve; TC, thermocouple; ϕ, phi (fuel-air) equivalence ratio.

* Corresponding author at: National Renewable Energy Laboratory, Attn: Jon Luecke, Mailstop 1634, 15013 Denver West Parkway, Golden, CO 80401, United States.
E-mail addresses: Jon.Luecke@nrel.gov (J. Luecke); Mohammad.Rahimi@nrel.gov (M.J. Rahimi); Brad.Zigler@nrel.gov (B.T. Zigler); Ray.Grout@nrel.gov (R.W. Grout)
[1] Equally contributed as first author.

https://doi.org/10.1016/j.fuel.2019.116929
Received 1 October 2019; Received in revised form 13 December 2019; Accepted 19 December 2019
Available online xxx
0016-2361/© 2019.

cludes a modern high-pressure piezoelectric diesel injector, minimizes spray physics effects to focus on chemistry effects, with greater temperature and pressure capability than other CVCCs. In non-premixed ignition, the processes of mixing and reaction are necessarily intertwined, and it is desirable to maximize the realism of the spray breakup to drive relevant mixture preparations. This is especially important for the cetane measurement of new (bio)fuels with physical properties that may fall outside the typical diesel-fuel range, in which cetane correlation shows dependence on injection technology [13]. However, for gasoline-range fuels, end-gas autoignition is a feature of interest, and to investigate the relevant longer ignition delays it is desirable to have a rapidly completed mixing process decoupled from subsequent chemical kinetics. Use of the AFIDA as a research platform in this regime is beyond its original intended purpose and extensive experimental characterization is necessary to determine guidelines for selecting an appropriate modeling approach.

Accurate chemical kinetic mechanism models are necessary to integrate with computational fluid dynamics (CFD) to enable numerical simulations of engine combustion, necessary for the development of advanced combustion engine strategies to increase efficiency and reduce emissions [14]. The selection of surrogate species to represent the complex real fuel is critical [15,16]. Development of chemical kinetic mechanisms for these surrogate species is challenging, requiring validation against experimental ignition data across a range of engine-relevant temperatures, pressures, equivalence ratios, and dilution [17,18]. Reductions of full kinetic mechanisms in terms of species and reactions are frequently necessary to enable engine combustion CFD with finite computing resources. Validations of both full and reduced kinetic mechanisms rely on experimental ignition data, most commonly from fundamental research devices including shock tubes, jet stirred reactors, and rapid compression machines [18]. More recently, the Ignition Quality Tester (IQT) CVCC has been used as a research platform to augment the data available from more fundamental research devices to provide ignition-delay data in complementary pressure and temperature regimes [19–23]. In general, shock tubes provide data at higher temperatures and lower pressures than engines. Rapid compression machines generally operate at low to intermediate temperatures and higher pressures, closer to an engine, but are normally limited to surrogate blends due to mixture preparation challenges [24–26]. While mixture preparation techniques have recently been developed for more complex surrogate blends in rapid compression machines and shock tubes, CVCCs can further extend these studies by providing fuel injection of complex, full-boiling-range liquid fuels [24,26,27]. While the ignition delay (ID) time in a CVCC is complicated by including physical effects along with chemical effects in the total ignition delay, deliberate operation and careful analysis of experiments can provide ignition delay data focused on the chemical ignition delay portion [28,29]. This can enable CVCC data to be used in CFD simulations to validate reduced kinetic mechanisms, and in some cases zero dimensional (0D) models can be used to evaluate full kinetic mechanisms. With the flexibility to handle complex real-world fuels, CVCCs can be research platforms to complement more fundamental devices to assist in the development of chemical kinetic mechanisms. Beyond developing chemical kinetic mechanisms, the ignition delay data from CVCCs and more fundamental devices can also be used to generate ignition delay maps to link with simpler engine simulations to study advanced combustion strategies [30]. To further advance the relevancy of CVCC combustion research, the National Renewable Energy Laboratory (NREL) acquired an AFIDA with the intent to similarly adapt it as a more flexible research platform for fuel ignition studies [31].

This paper presents a comprehensive characterization of the AFIDA device and an illustration of how it can be used in a research setting, combined with a complementary modeling approach to validate chemical kinetics mechanisms for the reference fuels 2,2,4-trimethylpentane and n-heptane, which exhibit both long and short autoignition delay times relative to the mixing timescale.

2. Materials and methods

2.1. Materials

The AFIDA instrument was purchased from ASG Analytik-Service Gesellschaft mbH. Millipore Sigma supplied the iso-octane (2,2,4-trimethylpentane 99.8% CAT# 360066), n-heptane (99% high-pressure liquid chromatography (HPLC) Plus Cat# 650536), toluene (99.8% anhydrous CAT# 244511), and ethanol (pure 200-proof CAT# 459844). Infineum International Limited supplied the R655 lubricity additive sample. Matheson Tri-Gas, Inc. supplied the certified 20.9% (molar volume) oxygen balance nitrogen air cylinders used for charge air. The analytical balance used was a Mettler Toledo PB303-S. A National Institute of Standards and Technology (NIST)-certified Omega DPG1001B-100G pressure gauge was used for external pressure measurements.

2.2. AFIDA overview

The AFIDA device directly injects fuel into a heated and pressurized fixed-volume combustion chamber and records pressure data to infer when the fuel autoignites. Fig. 1 shows the device installed at NREL, while Fig. 2 shows a simplified schematic of its key features. A 16-position auto-sampling system utilizing 40-mL sample vials and a sampling needle allows for continuous unattended operation. Fuel pressure up to 1200 bar is supplied by an HPLC-style pump consisting of two positive displacement piston pumps connected in series. Capillary stainless-steel lines connect the fuel pump to a Bosch CRI3-18-based piezoelectric diesel injector, which resides within a liquid-cooled housing that attaches to the top center of the combustion chamber using six spring-loaded bolts. Key injector parameters such as the symmetrical 143-μm 7-hole pattern and 79° spray angle geometry were provided by Robert Bosch LLC. The injection duration can range from 0 to 5 ms with up to four separate injection events possible. The operation of the fuel injector differs from a typical constant-pressure common rail injection system found on vehicles in that the HPLC fuel pump produces a very consistent initial pressure, but it does not respond while the injection occurs over the course of a few milliseconds. As a result, the pressure within the fuel system drops while the injection event occurs. While maximum fuel line pressure is limited by the fuel pump to 1200 bar, all experiments are carried out with an initial pressure of 1190 bar to avoid bumping against the limit. An injection duration of 4 ms leads to the fuel line pressure dropping to near 250 bar. The coolant, which surrounds the injector excluding the tip and rear electrical connection portion, is held at a temperature of 338 K ± 5 K. To prevent any possible boiling issues for volatile fuels, the pressure of the fuel system never drops below 50 bar once the injector is purged of fuel, even while idle. The return line of the fuel injector has an adjustable back-pressure regulator typically set to 17.5 bar and plumbed to a waste container. The mostly cylindrical (approximately 4-cm height by 5-cm radius) combustion chamber is heated around the perimeter via a band heating element up to a maximum internally measured air test temperature of 998 K, measured using the average of two equidistant off-center class 2, type K (nickel-chromium/nickel-alumel) thermocouples mounted within the bottom of the combustion chamber. Pressure data from a liquid cooled Kistler 6041B pressure transducer, also mounted at the bottom of the combustion chamber, begins recording at 250 kHz from moments before the injection event occurs through 40 ms. For experiments leading to ignition delays exceeding 40 ms, the sampling rate is reduced to 25 kHz for a user-specified time. Two separate regulated gas inputs feed through Bronkhorst 201CV and/or 201AV mass flow controllers (MFC) to allow precise filling of the chamber to pressures ≤50 bar.

Fig. 1. AFIDA device installed at NREL.

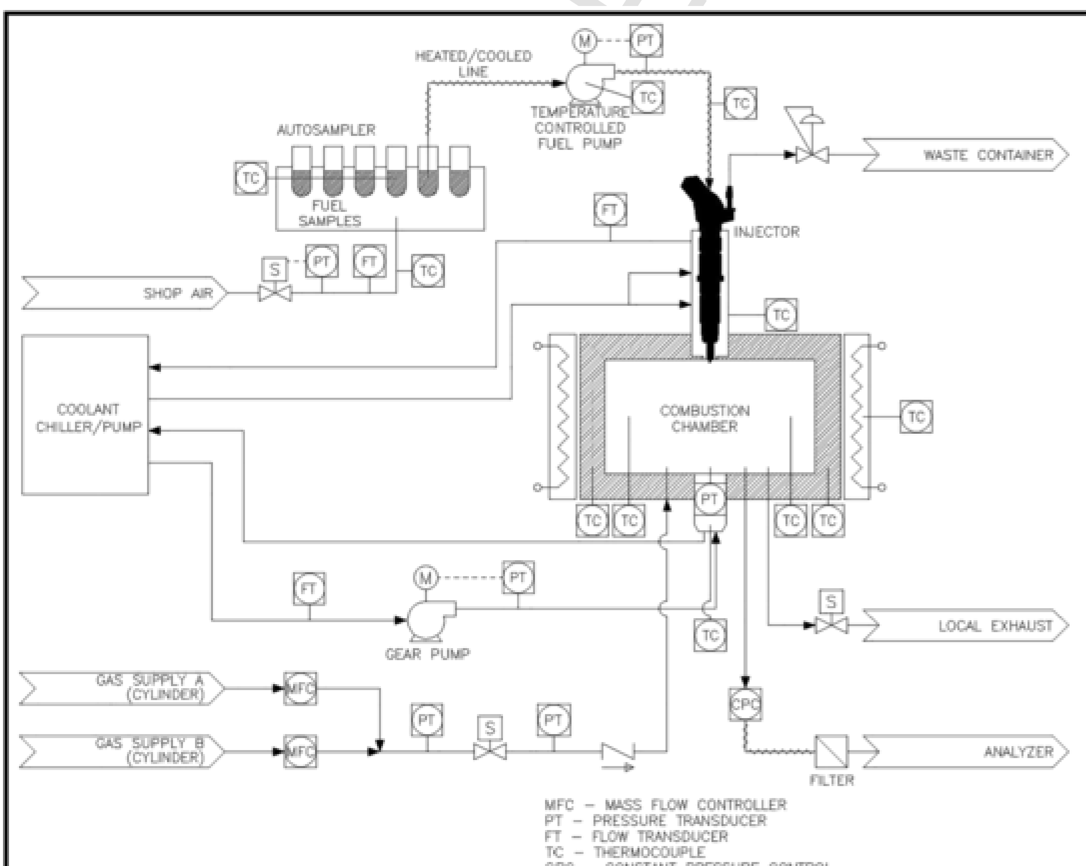

Fig. 2. AFIDA schematic.

2.3. Experimental test sequence

A test sequence begins by purging the low-pressure area of the fuel system with the new fuel sample, achieved by actuating the injector at a rate of 50 Hz while running the HPLC pump, resulting in 20 to 40-bar pressure conditions throughout the fuel system and injector. This process takes 420 s and uses approximately 20 mL of fuel to flush all the lines, the fuel reservoir mounted atop the injector, and most areas within the fuel injector. A smaller volume of fuel was found to adequately purge the fuel system, but typical setpoints here were maintained as fuel volume was not limited. Next, the internal area within the tip of the injector, which cannot be purged without injecting fuel, is purged using a series of 18 actual injections. Once complete, two fully sequenced pre-injections are performed, followed by 12 injections which are recorded. The combustion sequence begins by flowing charge air gas through the chamber directly to exhaust at approximately 3 bar to both cool the chamber below the test temperature setpoint and remove residual exhaust gas. Once the chamber is cooled 5 K below the test temperature setpoint, the exhaust valve closes and the chamber pressurizes to the setpoint. During the chamber charging process, the fuel pump pressurizes the fuel line to the setpoint. Injection occurs as the following three conditions are simultaneously met: the chamber temperature is within 0.5 K of the test temperature setpoint, the chamber air pressure is within 0.5 bar of the test pressure setpoint, and the fuel line pressure is within 5 bar of the fuel pressure setpoint. When the criteria are met, the locking (isolation) valve closes to completely seal the chamber and shield the mass flow controllers, and the pressure transducer signal is recorded at 250 kHz starting 0.4 ms before the injection event is electronically triggered. The fuel line pressure and chamber air pressure setpoint are typically maintained before the temperature setpoint is reached, resulting in the chamber temperature parameter controlling the timing of the injection event. This control strategy allows for very repeatable control of injection event timing as it relates to the temperature history profile of the charge air before injection. The entire process of a fuel purge and ignition delay measurement takes around 20 min, although subsequent tests using the same fuel without the need for purging require only 9 min to complete. The AFIDA's indicated cetane number test run as per ASTM D8183 has a slightly different fuel purge sequence, although the combustion sequence is identical [5].

2.4. Numerical methods

Two separate approaches are used to model the AFIDA process: a homogenous reactor based on a zero-dimensional (0D) formulation that considers only chemical kinetics, and a three-dimensional (3D) computational fluid dynamics (CFD) model that includes the spray and mixing physics in conjunction with the chemical kinetics.

The homogeneous reactor model of the device to predict ID times is performed using a Python interface to the open-source kinetic modeling software Cantera [32]. The system is modeled as a constant-volume batch reactor with the initial temperature, pressure, and mixture composition matching the experimental conditions.

The 3D modeling is performed using the CONVERGE CFD software package [33]. The conservation equations are solved using a second-order accurate finite volume method with first-order implicit time accuracy. Pressure-velocity coupling in the transport equations are solved by the Pressure-Implicit with Splitting of Operators method. Variable time stepping using a Courant-Friedrichs-Lewy number less than 0.5 is used for calculation of each time step. The solver uses Lagrangian-Eulerian coupling to treat the discrete spray parcels in the continuous gas phase. A "blob injection method" [34] is used for spray injection, modified Kelvin-Helmholtz and Rayleigh-Taylor models [35,36] are used for droplet breakup, the No-Time-Counter model [37] is used for droplet collision, the Frossling model [38] is used for droplet evaporation, the Dynamic Drag model [39] is used for droplet drag effect, and the O'Rourke model is used for droplet turbulent dispersion. Renormalization group k-epsilon Reynolds-Averaged Navier-Stokes was used for modeling turbulence. The cut-cell Cartesian method used in the software automatically creates an orthogonal computational grid that precisely represents the geometry from a computer-aided design description. The internal base grid size is 1 mm initially and the areas with high gradients are automatically refined using adaptive mesh refinement based on the velocity and temperature fields. The smallest grid size in cases of highest refinement was 0.125 mm (three levels of refinement). To resolve flow near the injector, a fixed nozzle embedding was used during the spray injection time with a minimum grid size of 0.125 mm, which provides enough detail to achieve accurate results with grid convergence [40]. This resulted in a peak cell count of about 5,000,000 at time steps with the highest refinement. A one-seventh slice of the symmetric AFIDA geometry consisting of one injector hole with periodic boundary conditions is used for the numerical reacting simulations. Each simulation case was run with 480 processors in parallel and computational costs varied from approximately 10,000–20,000 CPU hours. A graphical representation of the full geometry is depicted in Fig. 3, including the simulated one-seventh area slice and the initial mesh with injector embedding. The average internal temperature, discussed further in Section 3.1, is used for the initial condition within the CVCC. The injection duration of 4 ms matched the experiment. Injection volume, discussed further in Section 3.3, was experimentally measured and a constant injection flow rate over the duration was modeled. Table 1 shows the typical input parameters used for CONVERGE reacting simulations.

Chemical reactions are modeled directly using the SAGE detailed chemistry solver [41], which reads the chemical kinetic mechanism

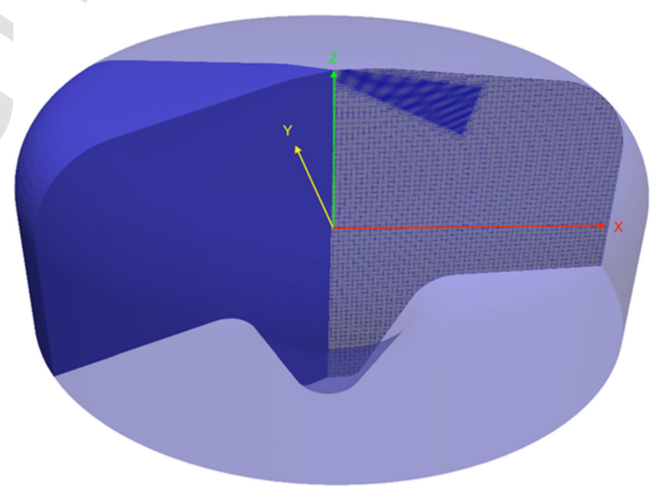

Fig. 3. Full AFIDA 3D geometry illustrating the simulated one-seventh area slice (left side) and the initial computational mesh with fixed near-nozzle embedding (right side).

Table 1
Parameters used for CONVERGE AFIDA simulations.

Fuel	n-heptane and iso-octane
Nozzle diameter	0.14 mm
Fuel mass injected	0.117 g
Injection duration	4 ms
Fuel temperature	363 K
Nozzle umbrella angle	79°
Nozzle embedding grid size	0.125 mm
Ambient temperature	973–648 K
Ambient pressure	10–20 bar (gauge)
Ambient composition	Air (20.9% molar volume O_2, balance N_2)

in CHEMKIN format. A reduced PRF mechanism with 127 species [42] derived from the Co-Optimization of Fuels & Engines (Co-Optima) detailed mechanism [43] was used for iso-octane and n-heptane 0D and 3D CFD simulations. Adaptive zoning was employed to accelerate the chemistry calculations.

3. Results and discussion

3.1. AFIDA temperature and volume characterization

To characterize temperature stratification within the combustion chamber, a 1/8-inch type K thermocouple was inserted through an exhaust port and temperatures from top to bottom were measured at 11 locations along the z-axis, as shown in Fig. 3, and at 9 locations along two other outer radial positions, as illustrated in Fig. A.1. This was done for AFIDA specified "test temperature" conditions ranging from 998 to 673 K in 50-K increments at 10 and 20 bar, measuring temperature immediately before injection occurs. These data points, along with wall temperature measurements taken from two type-K thermocouples present in the CVCC (seated within the chamber wall), were used to build a detailed model representing the temperature stratification present with the chamber, shown in Fig. A.1. There is approximately 10 K of temperature stratification present throughout most of the combustion chamber when pressurized, less than the magnitude present at unpressurized steady-state conditions. From this model, the average internal temperature was calculated and found to be 25 K lower than the AFIDA specified "test temperature." Ignition delay results are plotted and modeling is performed using the calculated average internal temperature. For example, if the AFIDA's test temperature was set to 998 K, the ignition delay results are plotted using a temperature of 973 K, and corresponding 0D and 3D CONVERGE simulations use an input temperature of 973 K.

The moles of air present within the CVCC was measured at 5, 10, and 20-bar pressure (reported as gauge pressure throughout this document) at room temperature by evacuating the pressurized CVCC volume into a 2.795-L vacuum-filled SUMMA canister. Pressure was recorded using a NIST-certified pressure gauge and moles were calculated using the ideal gas law. The total moles measured, which includes the moles of air present in the canister along with an estimation of the moles of air left in the CVCC chamber, were within 3%–5% of the moles predicted by the CFD model depending on pressure, which verified model geometry accuracy. This procedure was also performed at 673 K and produced agreement within 10%. There is some temperature uncertainty in this technique, especially when attempting to measure the volume of a high temperature charge, resulting from the gas expanding into the SUMMA canister while heating simultaneously occurs within the combustion chamber.

3.2. Piezoelectric injector operability using gasoline-range fuels

The use of gasoline-range fuels throughout the fuel system poses challenges not present when using diesel fuels, for which the device was originally intended. There are very little data regarding the use of gasoline fuels with piezoelectric diesel injectors, and there are reasonable issues to consider. Piezoelectric diesel injectors use the fuel internally as part of the hydraulic amplification system attached to the movement of the piezo stack, which ultimately opens the injector. In general, sealing gasoline-range fuels within the high-pressure fuel system is more difficult than diesel fuels due to the decreased viscosity. The possibility of cavitation caused by either fuel boiling or pump pressure differentials is significantly higher when using fuels with much higher vapor pressures such as gasoline-range fuels.

The addition of a lubricity additive proved to be helpful in restoring well-controlled injection operation with n-heptane and iso-octane. An evaluation was performed to determine the correct amount of lubricity additive to add to iso-octane to maximize injector operability while minimizing the perturbation of the combustion kinetics. Without the use of the additive, normal injector operation was found to be somewhat sporadic. The problems experienced included irregularities in shot-to-shot injections, as evidenced by the measured pressure trace and ID time, increased variability of gravimetrically measured fuel delivered (discussed further in Section 3.3), and occasional internal leaking from the high-pressure side of the injector to the low-pressure side. These anomalies have origins with the control valve and nozzle module, the two moving parts within the injector likely influenced by a lack of lubricity. The lubricity additive also helped ease sticky fuel pump inlet check valve operation issues that occasionally present in HPLC pumps.

Based on prior research using gasoline in diesel engine platforms, Infineum R655 was considered [44]. ID times measured at $\phi = 0.8$, 823 K, 10 bar conditions for Infineum R655 blended into iso-octane at levels ranging from 0 to 1500 parts per million by volume (ppmv) are shown in Fig. 4, using four different ignition delay definitions discussed further in Section 3.4. ID times clearly trend downward from 0 to 750 ppmv levels and stabilize at 1000–1500 ppmv levels, while the corresponding average peak combustion pressures shown in Fig. 5 trend upward from 0 to 750 ppmv levels and stabilize at 1000–1500 ppmv levels. As lubricity additive levels are increased, injector functionality improvements both increase and stabilize fuel injection volumes, thereby increasing global ϕ and reducing ID time, along with producing higher peak combustion pressures. Since the lubricity additive itself is not designed to influence fuel reactivity, the majority of the relatively small 7% decrease in ID observed between iso-octane with no additive and iso-octane with 1000 ppmv R655 additive is likely due to fuel delivery improvements, supported by peak combustion pressure data. Based on this information, the doping level of 1000 ppmv R655 was used in all fuel samples used during this study, excluding diesel fuel, which allowed for continuous operation using n-heptane and iso-octane fuel samples without experiencing injection functionality issues due to lubricity deficiencies. This 0.1% by volume blend level is comparable to the purity level of fuels used in the study.

3.3. Injection volume characterization

Although this study focuses primarily on a single injection duration of 4 ms for n-heptane and iso-octane—fuels which have similar physical properties and therefore exhibit similar injection profiles—it is interesting to note how the piezoelectric injector performs for a wide variety of liquid fuels. In addition to more extensive characterization of the fuel volume delivered for iso-octane and n-heptane with a 4-ms duration, the injector's delivered fuel volume was measured for five different fuels over eight different injection durations by injecting fuel into a closed tube fit tightly over the tip of the injector and weighing the collected fuel with an analytical balance. The weight of fuel was then converted to volume using the density of the fuel. The five fuels with different physical properties calibrated were certification diesel fuel, iso-octane, ethanol, toluene, and a full-boiling-range gasoline (a renewable blendstock for oxygentate blending (RBOB) used in the Co-Optima program) [45]. This procedure was done twice for each data point, with the average result plotted in Fig. 6, in addition to 10 measurements done each for iso-octane and n-heptane at 4 ms duration, which are nearly identical. The repeatability of the weight measurement was excellent, with the RBOB gasoline fuel presenting the worst repeatability with a 2.3% measured weight difference between measurements at a 0.5-ms duration, and most fuels presenting within 0.2% of each other. Noticeable differences in injection volumes were measured between the fuels, as iso-octane flowed at the fastest rate of 169 μL per injection with a 4 ms duration while the certification diesel flowed at 143 μL per injection, likely a result of the physical property differences (viscosity, density, and bulk modulus) between the fuels.

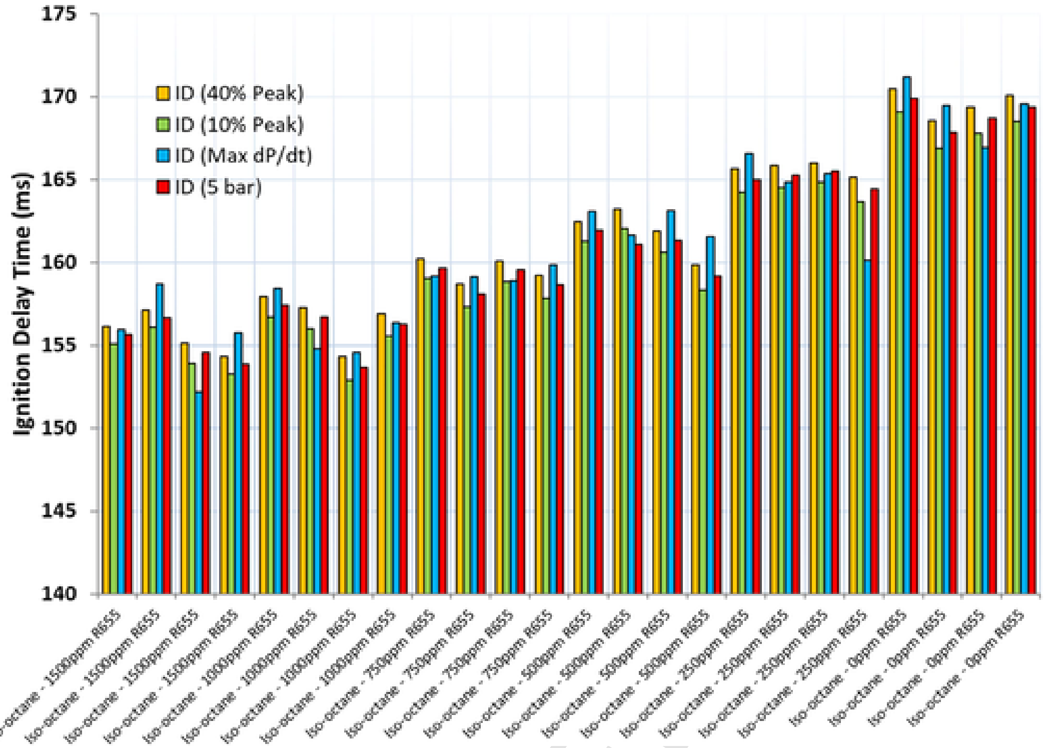

Fig. 4. Comparison of ignition delay time results (using four different ignition delay definitions) for various lubricity levels in iso-octane at $\phi = 0.8$, 823 K, 10 bar conditions.

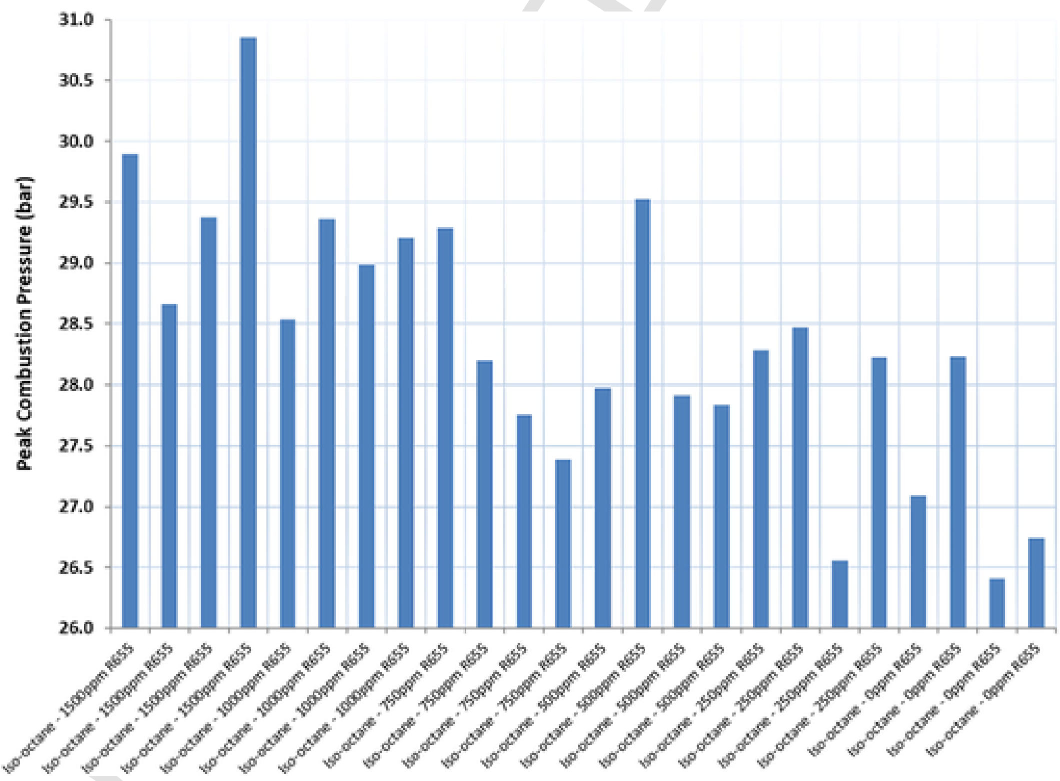

Fig. 5. Comparison of average peak combustion pressure for various lubricity additive levels in iso-octane at $\phi = 0.8$, 823 K, 10 bar conditions.

3.4. Ignition delay time definition

Ignition delay time is defined here as time elapsed between the start of injection and the start of combustion. The start of injection is simple to identify from the pressure transducer data, whereas the start of combustion has more ambiguity in its definition, although repeatable identification is possible based on various definitions, including maximum rate of pressure rise, absolute pressure thresholds, and fractions of peak pressure.

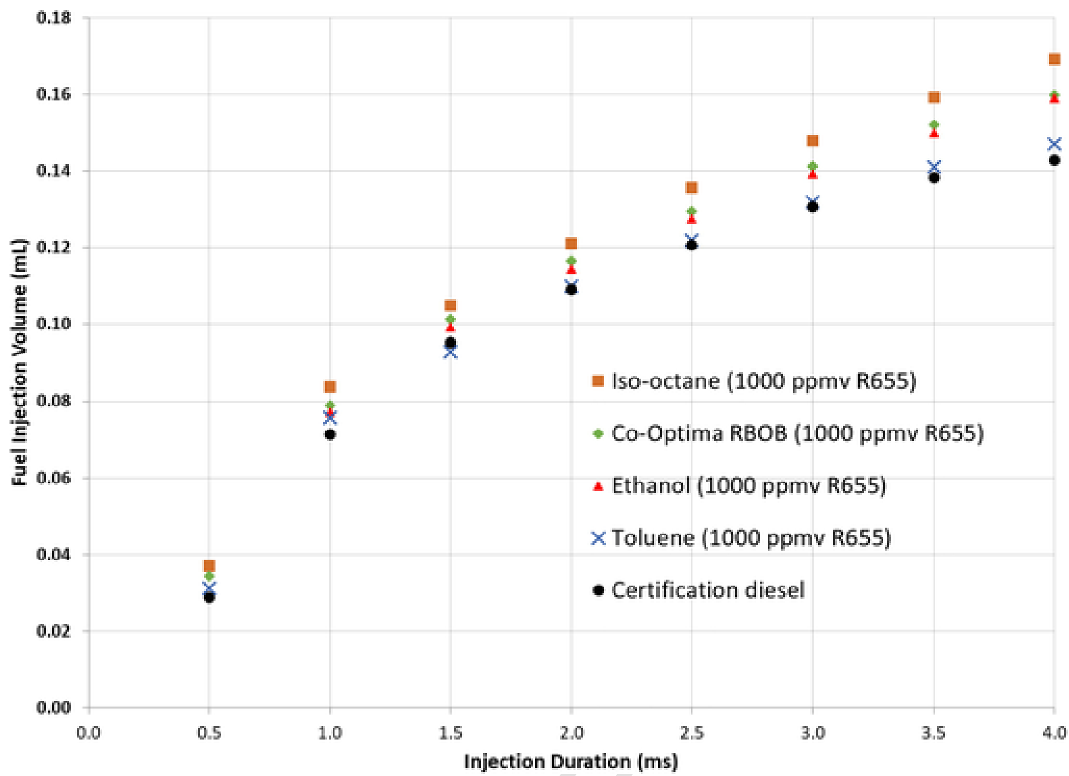

Fig. 6. Measured injection volumes for various fuels.

Before fuel is injected into the chamber there is a very short electronic triggering delay followed by a hydraulic delay within the injector. This total time of 0.12 ms (which includes both the electronic and hydraulic delay times) is extremely repeatable as long as the system is not altered. The pressure transducer begins picking up noise at the precise moment fuel begins to enter the combustion chamber, which defines the start of injection.

A thermodynamic approach defines the start of ignition as coinciding with the maximum apparent heat release rate, which is the rate of heat release consistent with the observed pressure change, neglecting heat transfer and assuming ideal gas behavior. This is measured by the maximum slope of the pressure trace (max. dP/dt). This measure was observed to be quite sensitive to noise in the pressure signal as well as changes in the combustion mode. A seven-point moving average was applied to the raw pressure data to smooth it, making calculation of max. dP/dt less noisy.

Another approach commonly used with CVCCs is to define the start of ignition where the pressure trace exceeds a specific threshold. This simple and consistent methodology is used within various ASTM methods to correlate a measured ID time to a cetane number [4]. Under those circumstances, however, there is typically no low-temperature heat release (LTHR) occurring due to the carefully chosen conditions under which they are run for diesel fuels, but this is not the case for gasoline-range fuels, which react slower and become more well mixed before ignition. The threshold concept has the advantages of being both simple to apply to a data set and extremely consistent. Over wide pressure and temperature operating conditions, however, care must be taken to choose the correct threshold to properly measure LTHR, high-temperature heat release (HTHR), or both, and a single threshold may not work well for an experiment covering a wide pressure and temperature range. A 5-bar pressure threshold was one ignition delay definition used in this study to calculate ID times.

Under some conditions certain fuels may undergo two-stage ignition involving an initial pressure rise due to LTHR, or "cool flame," combustion kinetics, which can occur well before the HTHR event [46]. Especially in these cases, it is important to distinguish between the ID time resulting from either LTHR or HTHR. For diesel-range fuels, previous work in CVCCs has noted that first-stage ignition produces approximately 10% of the pressure rise ultimately associated with the premixed burn following ignition [47]. We report ignition delay based on two relative pressure thresholds at 10% and 40% of measured peak pressure for the ignition event. This definition is robust and works well for all conditions studied. For many cases, the 10% peak and 40% peak definition produces very similar ID times since the HTHR ignition event typically produces a very large slope. The 10% peak definition could potentially trigger in cases where significant LTHR is present, while the 40% peak definition will generally always pick up the HTHR ignition. The pressure recovery point and maximum pressure drop are also recorded as part of an algorithm developed to process AFIDA pressure data quickly.

Table 2 shows a comparison of the various ID definitions and how they apply to an iso-octane 20-bar temperature sweep from 973 to 648 K average internal temperature where ϕ varies from 0.6 to 0.4, while a plot of this data is found in Fig. A.2. Here, all ID definitions produce very similar results except in the low-temperature areas, where the 10% peak definition picks up the LTHR pressure increase and the others do not. Fig. 7 graphically illustrates the difference in all previously discussed ID time definitions with an example of iso-octane ignition at 20 bar, 648 K, $\phi = 0.4$ conditions.

3.5. Mixture stratification characterization

Characterizing the spray physics and mixing associated with these experiments is critical to understanding the fuel/air ratio stratification and facilitating identification of a timescale over which the physical effects such as spray injection, evaporation, and diffusion are large influences on overall ID time compared to the chemical kinetics. For observed IDs significantly longer than the period over which local fuel/air ratio stratification dissipates, chemical kinetic pathways are expected to dominate. A CFD simulation of the mixing process (with chem-

Table 2
Ignition delay time comparisons of iso-octane 20-bar data.

AFIDA average internal temperature (K)	Temperature (1000/K)	Global ϕ	ID (max. dP/dt)	ID (5-bar threshold) (ms)	ID (40% peak) (ms)	ID (10% peak) (ms)
973	1.03	0.61	14.2	13.9	14.1	13.7
948	1.05	0.59	17.9	17.2	17.8	16.8
923	1.08	0.58	23.8	21.9	22.7	21.5
898	1.11	0.56	30.6	29.8	30.2	29.4
873	1.15	0.55	35.2	34.7	35.1	34.3
848	1.18	0.53	37.4	36.7	37.0	36.3
823	1.22	0.52	37.5	37.0	37.3	36.6
798	1.25	0.50	37.0	36.4	37.0	35.9
773	1.29	0.48	36.1	35.0	35.9	34.3
748	1.34	0.47	35.9	33.7	35.0	32.7
723	1.38	0.45	35.5	34.0	35.6	32.5
698	1.43	0.44	44.4	41.9	44.0	38.4
673	1.49	0.42	59.3	55.6	58.4	40.7
648	1.54	0.41	95.4	85.4	94.2	68.1

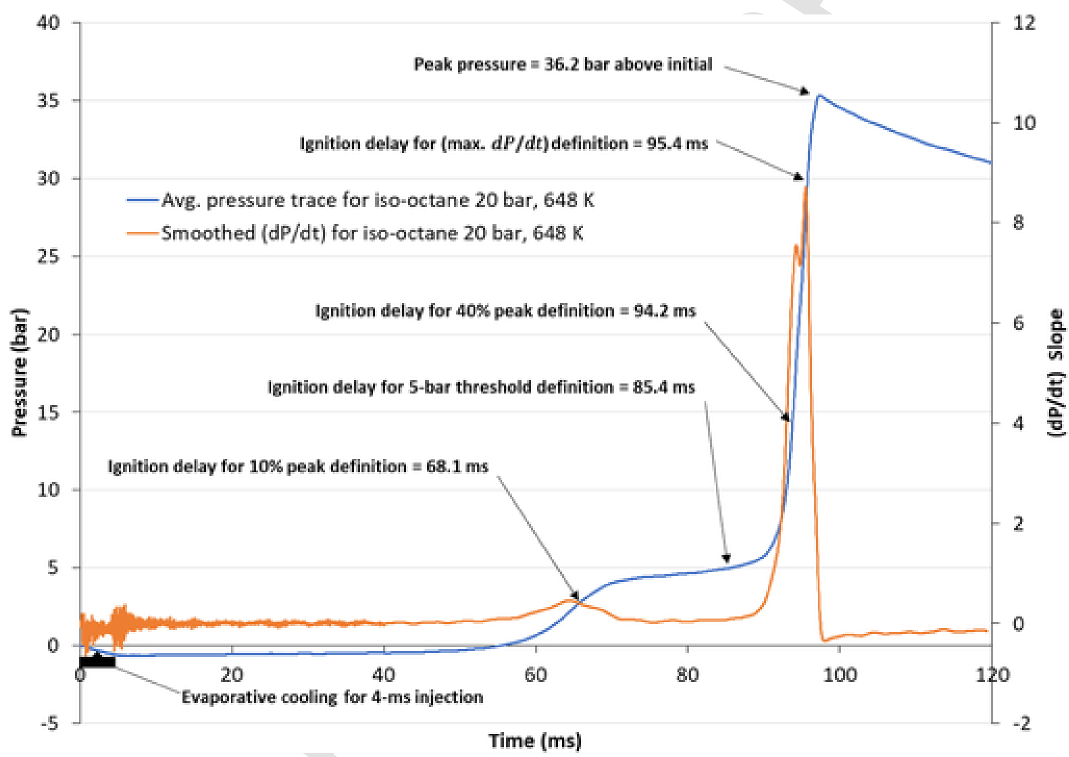

Fig. 7. Ignition delay definition comparison for iso-octane at 20 bar, 648 K test temperature, ϕ = 0.4.

istry deactivated) is used to study the physics of the injection event. Fig. 8 shows the simulated fuel/air ratio stratification for an injection of iso-octane at 10 bar and 973 K test temperature within the device at 1, 3, 5, 10, 30, and 50-ms timesteps. The total amount of fuel injected in the simulation was 0.169 mL over a 4-ms duration. Large local fuel/air ratio stratification exists through 5 ms, but by 10 ms the only completely unmixed fuel/area is in the lower region, which houses the pressure transducer. By 30 ms the concentration is quite uniform outside of the region near the pressure transducer and difficult to distinguish from that of 50 ms. Concentration gradients for the same conditions across the AFIDA x-axis (see Fig. 3) are extracted in Fig. 9, where the five lines each represent a specific time after the start of injection and show the predicted iso-octane mole fraction concentrations starting at the center of the AFIDA and proceeding radially towards the outer boundary. Simulations at 10 bar, 673 K and 20 bar, 798 K conditions yielded similar results, as shown in Figs. A.3 and A.4. This analysis suggests that the AFIDA becomes very well mixed by 30 ms after injection, and the physical effects of spray evaporation and mixing are not expected to be very influential from this point on.

3.6. Experimental uncertainty analysis

The key parameters to understand for this experimental setup are pressure, temperature stratification within the combustion chamber, ϕ, and the definition of ignition delay time. Each of these parameters has been experimentally characterized and examined, and all experimental data reported show error bars which are set at 95% confidence intervals based on a summation of both the experimental error of ignition delay measurement of twelve individual injections and all of the possible error within the initial conditions resulting from fuel delivery and measurement (temperature/pressure) uncertainty.

The liquid-cooled Kistler 6041B pressure transducer has specifications of 0.3% full-scale linearity on 250 bar, thus absolute accuracy falls within ±0.75 bar for any given reading. This error is associ-

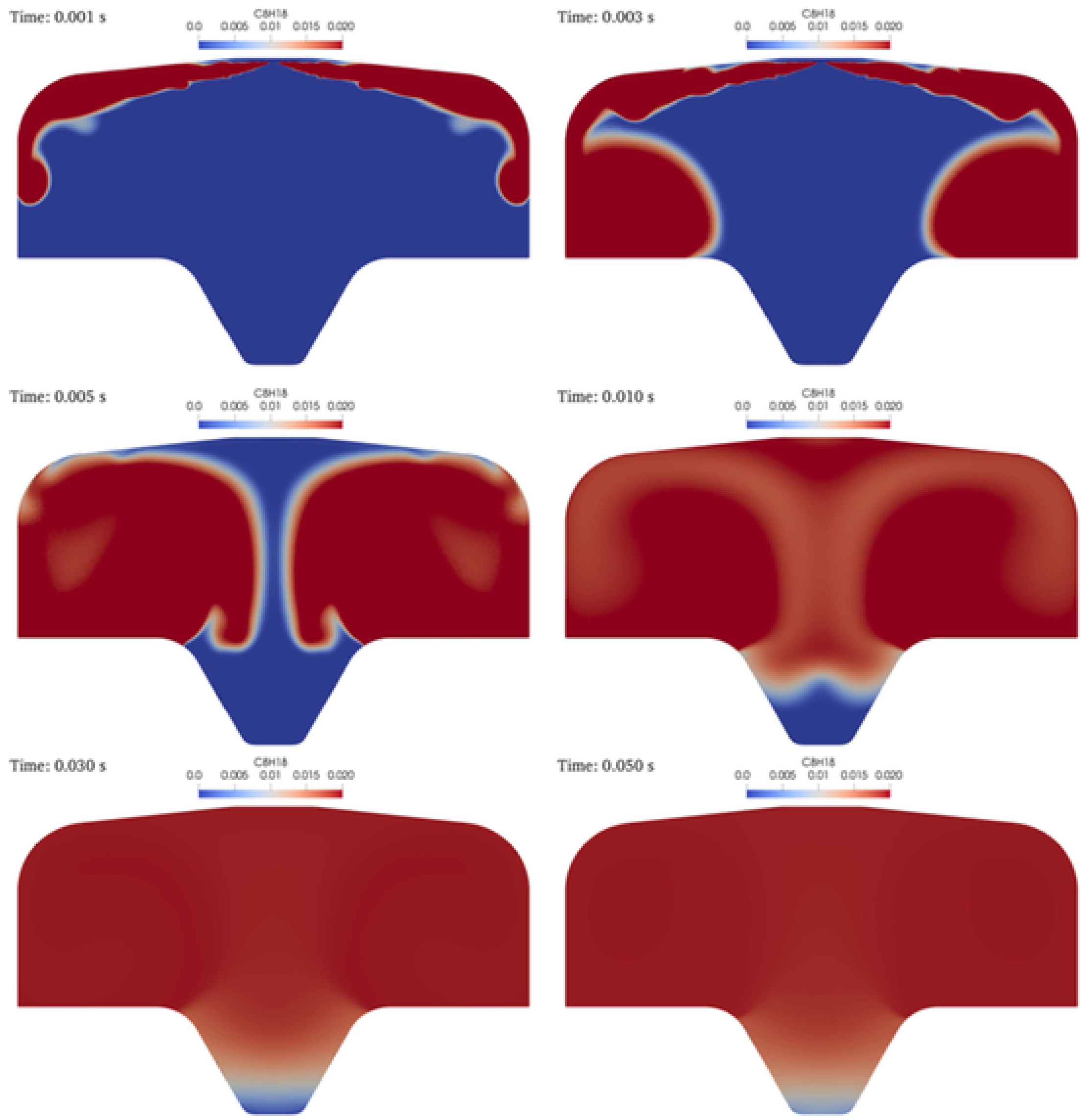

Fig. 8. Nonreacting CFD simulation showing iso-octane mole fraction present in the AFIDA for $\phi = 1.2$, T = 973 K, and P = 10 bar.

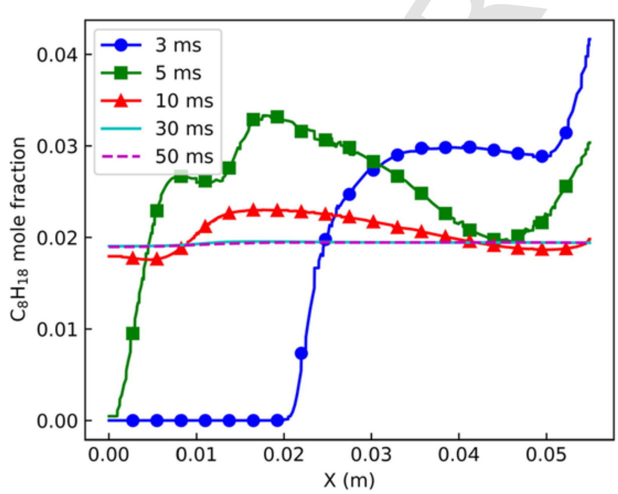

Fig. 9. Simulated iso-octane mole fraction concentration starting from the center (X = 0) and moving radially outward on the AFIDA's x-axis (see Fig. 3) for $\phi = 1.2$, 973 K, 10 bar conditions with a 4 ms, 0.169-mL injection, centered on the y and z axes.

ated with initial pressure conditions and pressure rise measurements. Global fuel/air ratio is calculated from the amount of fuel and moles of air present in the combustion chamber. As expected, the piezoelectric diesel injector produces extremely repeatable injection volumes, which were experimentally measured, with injection-to-injection measurement variances gravimetrically measured to be 0.169 mL with a standard deviation of less than 0.0004 mL for iso-octane with a 4.0-ms injection duration. The calculation of moles of air present is based on the volume and average internal temperature within the combustion chamber. Volume is calculated from the mesh, created from ASG Analytik-Service Gesellschaft mbH-supplied engineering drawings. The moles of air within the combustion chamber is calculated using a CFD model based on temperature measurements taken within the combustion chamber at various locations. Temperature measurements taken using standard class 2, type K thermocouple have accuracy within ±2.2 °C or 0.75% (of the reading in °C), whichever is greater. An estimation of the modeling error is not included here but the maximum thermocouple error for the measurements recorded from which the model is built was considered. The maximum error associated with initial moles of air and fuel was used to calculate the maximum error in global fuel/air ratio. The 0D Cantera batch reactor model was then used to estimate the maximum error of the ID time as a function of maximum temperature error, initial pressure error, and maximum global ϕ error. Once this error was generated, the 95% confidence experimental uncertainty was calculated based on the experimental standard deviation and applied to the maximum and minimum ID limits found using the 0D maximum error results. Table A.1 shows an example of how error bars were generated for two specific data points.

3.7. High-reactivity fuel: n-heptane results

Experimental measurements of ignition delay time for n-heptane were carried out at 10 and 20-bar pressures in 20.9% (molar volume) oxygen balance nitrogen atmosphere over the temperature range of 973–648 K. For the 10-bar experiment, global ϕ values were run close to stoichiometric ($\phi = 1.2 - 0.8$) from highest to lowest measured temperatures as injection duration was held constant. This range in global ϕ occurs if the injection duration is held constant due to ideal gas law calculations that result in less charge air present at higher temperatures, since pressure and volume are held constant. The data set for n-heptane was generated using approximately 150 mL of fuel over eight hours of unattended operation.

Figs. 10 and 11 compare experimental ID results versus numerical 0D and 3D CFD simulations for 10 and 20-bar experiments using the 127 species-reduced PRF Co-Optima mechanism mentioned earlier, while numerical ID prediction error quantification is shown in Fig. 12, plotting overprediction and underprediction of ID time as positive and negative error, respectively. Each experimental data point is the average of 12 measurements, with uncertainty error bars described in Section 3.6. 0D comparisons between the detailed and reduced PRF mechanisms showed no significant difference in ID time predictions or negative temperature coefficient (NTC) activity over the temperature and pressure conditions in this study (Figs. A.5 and A.6), and consequently the comparisons to the 0D detailed mechanism are left out for simplicity. Table A.2 contains all experimental ID data and standard deviations plotted in Figs. 10 and 11.

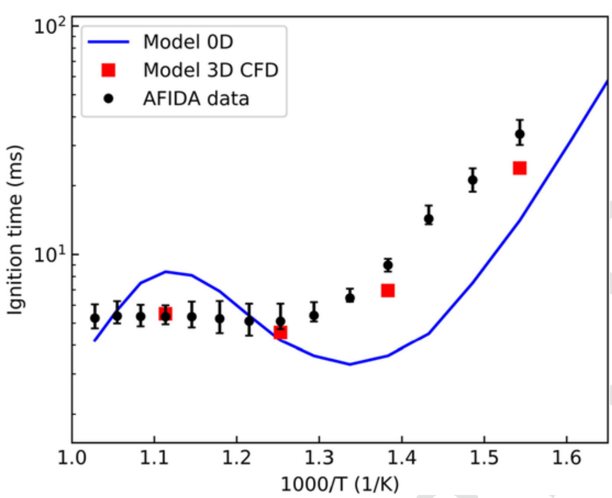

Fig. 10. Arrhenius plot showing experimental vs. numerical ignition delay results for 10-bar n-heptane over the temperature range (973–648 K) and global ϕ (1.2–0.8).

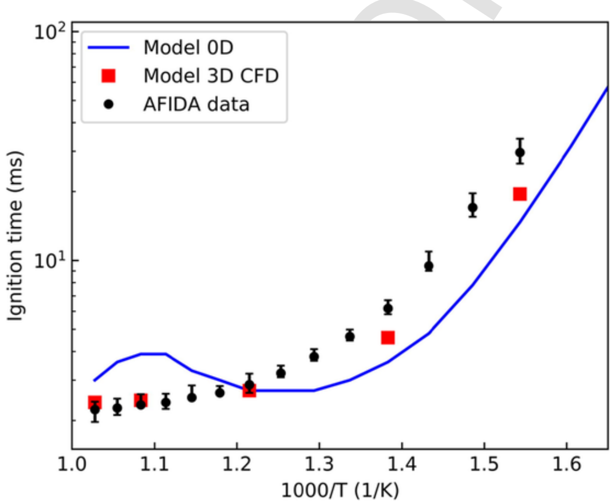

Fig. 11. Arrhenius plot showing experimental vs. numerical ignition delay results for 20-bar n-heptane over the temperature range (973–648 K) and global ϕ (0.6–0.4).

n-Heptane is very reactive and tests the limits of the experiment, as ID times at the higher temperature regions are extremely short compared to the injection duration of 4 ms. For the 20-bar experiment at 973 K, ignition occurs during injection, while for the 10-bar experiment, just over 1 ms of time elapses from the end of injection to the start of ignition. Maximum error between experimentally measured ID time data vs. 0D numerical simulations for both 10 and 20-bar cases ranges from approximately $\pm 60\%$, and the experiment loses the ability to capture the full magnitude of NTC chemistry predicted from 0D simulations under these conditions. A discrepancy between 0D and measured ID data is expected due to the high level of ϕ stratification and physical mixing effects, conditions present in all but the lowest temperature data points, where the ID time is shorter than the time required for the fuel/air mixture to become homogeneous. For both 10 and 20-bar cases, the 0D model becomes more accurate at predicting ID time for the lower temperature experiments as the ID time increases. A noticeable level of NTC chemistry still presents in the experimental 10-bar n-heptane data, indicating important fuel combustion chemistry can still be observed in the ID times even while significant physical mixing effects are still occurring. This is a substantial improvement over previously reported similar IQT-based n-heptane autoignition experiments, where n-heptane NTC activity could not be observed at pressures above 2 bar at similar global ϕ [20]. The AFIDA's symmetrical geometry and higher fuel injection pressure leads to faster fuel/air mixing and increased observation of fuel chemistry effects on autoignition chemistry at shorter ID times versus IQT-based experiments. For the 20-bar case, where the magnitude of NTC activity is expected to decrease, all NTC experimental observation disappears.

The CFD model of the AFIDA captures the ignition delay times well in both cases, where total ignition delay time overlaps with the mixing timescale. The improvement relative to the 0D model is evident in both the absolute ID time prediction as well as the reduced magnitude of NTC chemistry effect and temperature shift. Throughout the entire temperature region explored for both 10 and 20-bar n-heptane data, the re-

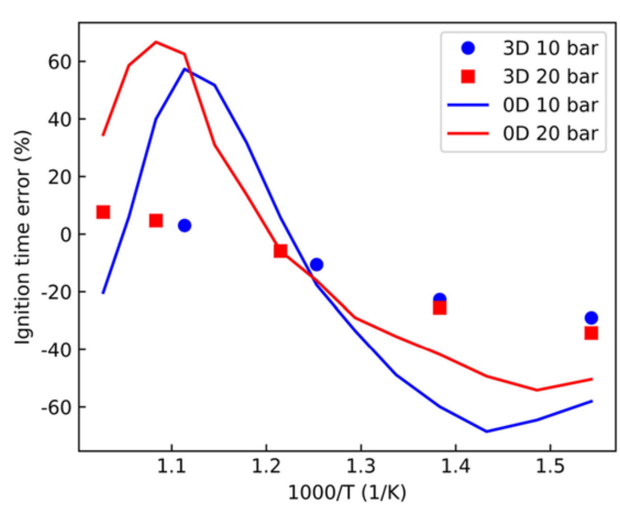

Fig. 12. Numerical n-heptane ignition delay time prediction percent error over temperature (negative error corresponds to underprediction of ID time).

duced kinetic mechanism only shows a maximum error of $+10\%$ to -30% in predicting the ignition delay, although error continues to increase at the lowest temperatures, indicating an opportunity to fine-tune the mechanism in these regions. Typical kinetic mechanism validation tools such as shock tubes and rapid compression machines do not operate at the lowest temperature regions used in these CVCC experiments, making it reasonable to find slightly more deviation there, where validation has likely not occurred. Experimental results are expected to become closer to 0D reactor predictions as temperature decreases and ID time lengthens, which is observed in the data plots for the lowest three temperatures.

These results indicate very good accuracy in the AFIDA CFD model, underscore the accuracy of the Co-Optima reduced kinetic model for n-heptane, and demonstrate the utility of the AFIDA to validate kinetic mechanisms for very fast-reacting fuels reasonably well using 0D approximation under mixing stratified conditions, although the use of CFD is required for more accurate comparisons in this case, especially as related to NTC activity.

3.8. Low-reactivity fuel: iso-octane results

Experimental measurements of ID time for iso-octane under the same pressures, temperatures, and stoichiometry used for n-heptane are presented along with the corresponding simulations in Figs. 13 and 14, while a chart quantifying numerical ID prediction error is shown in Fig. 15. This includes 10-bar ($\phi = 1.2 - 0.8$) and 20-bar ($\phi = 0.6 - 0.4$) experiments using 20.9% oxygen balance nitrogen atmosphere over the test temperature range of 973–648 K. Table A.3 contains all experimental ID data values and standard deviations that have been plotted in Figs. 13 and 14.

As with the n-heptane results, a large discrepancy (–75%) in 0D ID times versus experimental occurs at the highest temperatures. Again, this is as expected due to large ϕ stratification found within the combustion chamber at those conditions that is not accounted for in the 0D model. The ID prediction error for 0D versus experimental decreases as the ID time increases, and for ID times over 50 ms for both 10 and 20-bar data, error floats between $\pm 25\%$, except for the lowest temperatures, where error continues to increase, illustrating an area of possible mechanism improvement. For fuels exhibiting longer ID times such as iso-octane, a 0D modeling comparison versus experimental data is a reasonable check on mechanism accuracy.

The CFD model can accurately account for the physical effects and captures the ID in the high temperature region to within around 10% absolute error for both pressure cases. Once the ID times become long enough, the ID times predicted by the CFD model approach the 0D result. The 10-bar case takes a slightly longer time for the 0D and CFD to converge (around 60 ms), compared to the 20-bar case where the results are similar for IDs over 30 ms. This may be due to increased injection turbulence and mixing present in the 20-bar case. For the 10-bar case, the CFD does correctly shift the temperature location for NTC onset to slightly higher temperatures, which the 0D model misses. For the 10-bar condition, both 0D and CFD models predict slightly longer ignition delays (20%–40%) throughout the NTC chemistry areas than is seen experimentally. There is larger disagreement between 3D modeling and experimental data in the iso-octane 20-bar case compared to the 10-bar case. The most significant deviation begins around the area where NTC chemistry begins, where both the 0D and 3D CFD simulations markedly underpredict the level of NTC chemistry magnitude here and miss the extent of temperature space affected by NTC activity compared to the experiment. ID times here are between 30 and 40 ms, where the system is quite homogeneous. This suggests an opportunity to improve the Co-Optima detailed mechanism and corresponding reduced PRF mechanism within the NTC chemistry region over these pressure, temperature, and ϕ conditions.

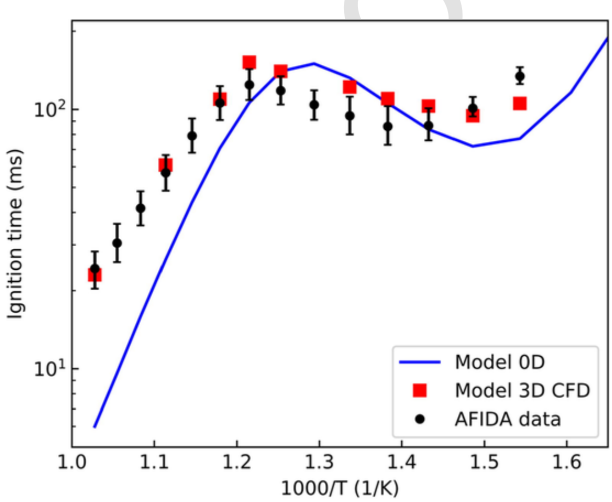

Fig. 13. Arrhenius plot showing experimental versus numerical ignition delay results for 10-bar iso-octane over the temperature range (973–648 K) and global ϕ (1.2–0.8).

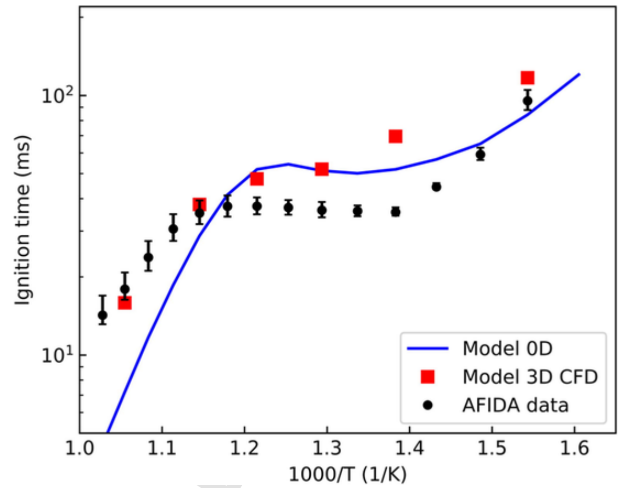

Fig. 14. Arrhenius plot showing experimental versus numerical ignition delay results for 20-bar iso-octane over the temperature range (973–648 K) and global ϕ (0.6–0.4).

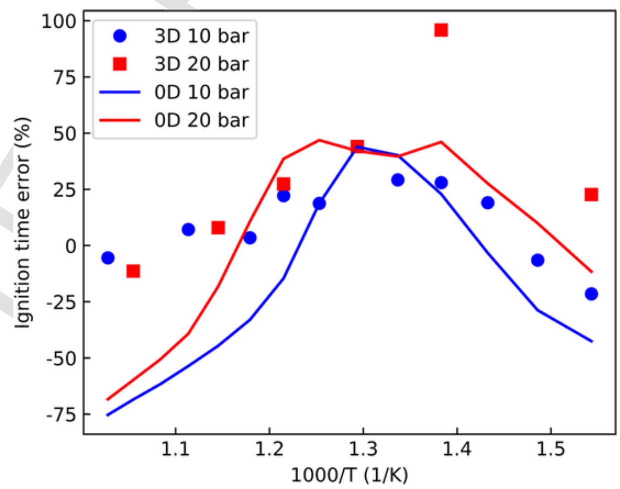

Fig. 15. Numerical iso-octane ignition delay time prediction percent error over temperature (negative error corresponds to underprediction of ID time).

4. Conclusion

NREL's newest CVCC, the AFIDA, is characterized in concert with complementary modeling to evaluate its potential to be used as a platform for validating chemical kinetic mechanisms for liquid fuels. Conditions studied include 14 different nominal test temperatures ranging from 973 to 648 K and pressures of 10 and 20 bar. Temperature uniformity was characterized experimentally by measuring wall temperatures and three radial positions with 10 axial measurements between the top and bottom. The injection volume delivered over various injection durations for the piezoelectric diesel injector was measured for four different gasoline-range fuels and a certification diesel fuel. This information, combined with very accurate pressure control using a high-fidelity pressure transducer, produced a well-controlled and characterized experiment for measuring a fuel's autoignition delay time in the AFIDA. A lubricity additive is useful at the level of 1000 ppmv to improve gasoline-range fuel performance of the piezoelectric diesel injector, with negligible impact on the measured ID.

Four different ID definitions were calculated from the AFIDA pressure data to determine differences introduced by the various techniques. A thermodynamic approach called max. dP/dt defines the start of combustion at the point of maximum measured heat release rate. A fixed relative pressure threshold of 5 bar was used as well. Neither of these approaches is universally applicable to the many pressure and temperature conditions that can sometimes produce significant LTHR profiles, whereas relative pressure measurements based on 10% and 40% of maximum pressure worked well at discerning LTHR and HTHR, respectively, at various pressure and temperature conditions.

A homogeneous model of the processes based on a Cantera batch reactor model, along with both detailed and reduced PRF mechanisms, resulted in reasonable agreement for ignition delay times >30 ms for iso-octane across 10-bar ($\phi = 1.2 - 0.8$) and 20-bar ($\phi = 0.6 - 0.4$) 973–648 K conditions. These delays correspond to conditions where the total ID is larger than the mixing timescale to achieve a homogeneous mixture within the AFIDA, estimated by a nonreacting CFD simulation of the injection process. There is significantly more error in the prediction from a homogenous model as ID times shorten, consistent with significant local air/fuel ratio stratification existing at time intervals closer to injection. In this regime, the physical influence of the spray injection, evaporation, and fuel/air mixing have a significant impact on ID time.

A CFD model of the AFIDA using CONVERGE software addresses the shortcomings of the homogeneous approximation by including spray physics and diffusion processes, as well as the chemical kinetics. CFD predictions of the ID using this model and a one-seventh simplified symmetry slice of the AFIDA geometry were within 25% of experimental ID measurements for most conditions. Experimental iso-octane ID time data over the NTC region indicate a larger magnitude of NTC activity compared to what the detailed and reduced PRF kinetic mechanisms predict, suggesting an area of opportunity to fine-tune the mechanism. From these data, informed decisions can be made on modeling requirements necessary for achieving desired accuracy of numerical ID predictions for a wide range of fuels exhibiting various experimental ID times within the device.

Using the AFIDA, small fuel volumes (150 mL) can be used to generate large quantities of autoignition delay data in hours for liquid fuels over wide temperature and pressure space but are limited to lean conditions for pressures >10 bar. 0D analysis of chemical kinetic mechanisms can be performed quickly as an initial indication of chemical kinetic model performance, which is especially useful at conditions that lead to ID times >30 ms. Chemical kinetic mechanisms can be evaluated more thoroughly over all pressure and temperature conditions using the CFD model, which captures the coupling between mixing physics and chemical kinetics throughout the experiment. The adaptation of the AFIDA as a flexible CVCC research platform strengthens the capability in the combustion research community for quickly evaluating chemical kinetic mechanism accuracy and evaluating fuel combustion quality for liquid fuels, including complex gasoline- and diesel-range blends.

Declaration of Competing Interest

The authors declare that they have no known competing financial interests or personal relationships that could have appeared to influence the work reported in this paper.

Acknowledgements

This work was authored by the National Renewable Energy Laboratory, operated by Alliance for Sustainable Energy, LLC, for the U.S. Department of Energy (DOE) under Contract No. DE-AC36-08GO28308. Funding provided by the U.S. Department of Energy's Office of Energy Efficiency and Renewable Energy, Bioenergy Technologies Office, and Vehicle Technologies Office. The views expressed in the article do not necessarily represent the views of the DOE or the U.S. Government. The U.S. Government retains and the publisher, by accepting the article for publication, acknowledges that the U.S. Government retains a nonexclusive, paid-up, irrevocable, worldwide license to publish or reproduce the published form of this work, or allow others to do so, for U.S. Government purposes. A portion of the research was performed using computational resources sponsored by the Department of Energy's Office of Energy Efficiency and Renewable Energy and located at the National Renewable Energy Laboratory.

This research was conducted as part of the Co-Optimization of Fuels & Engines (Co-Optima) project. Co-Optima is a collaborative project of several national laboratories initiated to simultaneously accelerate the introduction of affordable, scalable, and sustainable biofuels and high-efficiency, low-emission vehicle engines. The authors thank program manager Kevin Stork at the DOE Vehicle Technologies Office for supporting this research under the Co-Optima project.

The authors would also like to thank Philipp Seidenspinner at ASG Analytik-Service Gesellschaft mbH for his invaluable collaboration in adapting the AFIDA for fuel ignition kinetics research.

Appendix A. Supplementary data

Supplementary data to this article can be found online at https://doi.org/10.1016/j.fuel.2019.116929.

References

[1] N. Naser, S.Y. Yang, G. Kalghatgi, S.H. Chung Relating the octane numbers of fuels to ignition delay times measured in an ignition quality tester (IQT). Fuel 2017;187:117–127. doi:10.1016/j.fuel.2016.09.013.
[2] N. Naser, S.M. Sarathy, S.H. Chung Ignition delay time sensitivity in ignition quality tester (IQT) and its relation to octane sensitivity. Fuel 2018;233:412–419. doi:10.1016/j.fuel.2018.05.131.
[3] E. Polikarpov, K.O. Albrecht, J.P. Page, D. Malhotra, P.K. Koech, L. Cosimbescu, et al Critical fuel property evaluation for potential gasoline and diesel biofuel blendstocks with low sample volume availability. Fuel 2019;238:26–33. doi:10.1016/j.fuel.2018.09.129.
[4] ASTM International. ASTM D6890-18, Standard Test Method for Determination of Ignition Delay and Derived Cetane Number (DCN) of Diesel Fuel Oils by Combustion in a Constant Volume Chamber. West Conshohocken, PA: ASTM International; 2018.
[5] ASTM International. ASTM D8183-18, Standard Test Method for Determination of Indicated Cetane Number (ICN) of Diesel Fuel Oils using a Constant Volume Combustion Chamber—Reference Fuels Calibration Method. West Conshohocken, PA: ASTM International; 2018.
[6] ASTM International. ASTM D7668-17, Standard Test Method for Determination of Derived Cetane Number (DCN) of Diesel Fuel Oils—Ignition Delay and Combustion Delay Using a Constant Volume Combustion Chamber Method. West Conshohocken, PA: ASTM International; 2017.
[7] ASTM International. ASTM D613-18, Standard Test Method for Cetane Number of Diesel Fuel Oil. West Conshohocken, PA: ASTM International; 2018.
[8] CFR Engines Inc. CFR Engines Inc. Cetane Rating Unit, Model: F5, http://www.waukeshacfr.com/f-5/; 2019.
[9] A. Nicolle, N. Naser, T. Javed, N. Rankovic, S.M. Sarathy Autoignition characteristics of ethers blended with low cetane distillates. Energy Fuels 2019;33(7):6775–6787. doi:10.1021/acs.energyfuels.9b00571.
[10] G.E. Bogin Jr, J. Luecke, M.A. Ratcliff, E. Osecky, B.T. Zigler Effects of iso-octane/ethanol blend ratios on the observance of negative temperature coefficient behavior within the Ignition Quality Tester. Fuel 2016;186:82–90. doi:10.1016/j.fuel.2016.08.021.

[11] C.L. Barraza-Botet, J. Luecke, B.T. Zigler, M.S. Wooldridge The impact of physico-chemical property interactions of iso-octane/ethanol blends on ignition timescales. Fuel 2018;224:401–411. doi:10.1016/j.fuel.2018.03.105.

[12] Seidenspinner P, Härtl M, Wilharm T, Wachtmeister G. Cetane Number Determination by Advanced Fuel Ignition Delay Analysis in a New Constant Volume Combustion Chamber. SAE Technical Paper 2015;2015-01-0798. DOI:10.4271/2015-01-0798.

[13] M. Plank, G. Wachtmeister, K. Thuneke, E. Remmele, P. Emberger Effect of fatty acid composition on ignition behavior of straight vegetable oils measured in a constant volume combustion chamber apparatus. Fuel 2017;207:293–301. doi:10.1016/j.fuel.2017.06.089.

[14] C.K. Westbrook, M. Mehl, W.J. Pitz, G. Kukkadapu, S. Wagnon, K. Zhang Multi-fuel surrogate chemical kinetic mechanisms for real world applications. Phys Chem Chem Phys 2018;20:10588–10606.

[15] Pitz WJ, Cernansky NP, Dryer FL, Egolfopoulos FN, Farrell JT, Friend DG, Pitsch H. Development of an Experimental Database and Chemical Kinetic Models for Surrogate Gasoline Fuels. SAE Technical Paper 2007;2007-01-0175. DOI:10.4271/2007-01-0175.

[16] M. Mehl, J.Y. Chen, W.J. Pitz, S.M. Sarathy, C.K. Westbrook An approach for formulating surrogates for gasoline with application toward a reduced surrogate mechanism for CFD engine modeling. Energy Fuels 2011;25(11):5215–5223. doi:10.1021/ef201099y.

[17] S.M. Sarathy, G. Kukkadapu, M. Mehl, T. Javed, A. Ahmed, N. Naser, et al Compositional effects on the ignition of FACE gasolines. Combust Flame 2016;169:171–193. doi:10.1016/j.combustflame.2016.04.010.

[18] M. Mehl, W.J. Pitz, C.K. Westbrook, H.J. Curran Kinetic modeling of gasoline surrogate components and mixtures under engine conditions. Proc Combust Inst 2011;33(1):193–200. doi:10.1016/j.proci.2010.05.027.

[19] G. Bogin, A. Dean, M. Ratcliff, J. Luecke, B.T. Zigler Expanding the experimental capabilities of the ignition quality tester for autoigniting fuels. SAE Int J Fuels Lubr 2010;3(1):353–367. doi:10.4271/2010-01-0741.

[20] G.E. Bogin Jr, A. DeFilippo, J.Y. Chen, G. Chin, J. Luecke, M.A. Ratcliff, et al Numerical and experimental investigation of n-heptane autoignition in the ignition quality tester (IQT). Energy Fuels 2011;25(12):5562–5572. doi:10.1021/ef201079g.

[21] G.E. Bogin Jr, E. Osecky, M.A. Ratcliff, J. Luecke, X. He, B.T. Zigler, et al Ignition quality tester (IQT) investigation of the negative temperature coefficient region of alkane autoignition. Energy Fuels 2013;27(3):1632–1642. doi:10.1021/ef301738b.

[22] G.E. Bogin Jr, E. Osecky, J.Y. Chen, M.A. Ratcliff, J. Luecke, B.T. Zigler, et al Experiments and computational fluid dynamics modeling analysis of large n-alkane ignition kinetics in the ignition quality tester. Energy Fuels 2014;28(7):4781–4794. doi:10.1021/ef500769j.

[23] M. Tian, R.L. McCormick, J. Luecke, E. de Jong, J.C. van der Waal, G.P.M. van Klink, et al Anti-knock quality of sugar derived levulinic esters and cyclic ethers. Fuel 2017;202:414–425. doi:10.1016/j.fuel.2017.04.027.

[24] S.S. Goldsborough, S. Hochgreb, G. Vanhove, M.S. Wooldridge, H.J. Curran, C.J. Sung Advances in rapid compression machine studies of low- and intermediate-temperature autoignition phenomena. Prog Energy Combust Sci 2017;63:1–78. doi:10.1016/j.pecs.2017.05.002.

[25] X. He, M.T. Donovan, B.T. Zigler, T.R. Palmer, S.M. Walton, M.S. Wooldridge, et al An experimental and modeling study of iso-octane ignition delay times under homogeneous charge compression ignition conditions. Combust Flame 2005;142(3):266–275. doi:10.1016/j.combustflame.2005.02.014.

[26] D. Kang, A. Fridlyand, S.S. Goldsborough, S.W. Wagnon, M. Mehl, W.J. Pitz, et al Auto-ignition study of FACE gasoline and its surrogates at advanced IC engine conditions. Proc Combust Inst 2019;37(4):4699–4707. doi:10.1016/j.proci.2018.08.053.

[27] B.T. Fisher, J.C. Allen, R.L. Hancock, J.A. Bittle Evaluating the potential of a direct-injection constant-volume combustion chamber as a tool to validate chemical-kinetic models for liquid fuels. Combust Sci Technol 2017;189(1):1–23. doi:10.1080/00102202.2016.1193015.

[28] E.M. Osecky, G.E. Bogin Jr, S.M. Villano, M.A. Ratcliff, J. Luecke, B.T. Zigler, et al Investigation of iso-octane ignition and validation of a multizone modeling method in an ignition quality tester. Energy Fuels 2016;30(11):9761–9771. doi:10.1021/acs.energyfuels.6b01406.

[29] Suttle AE, Fisher BT, Parnell DR, Bittle JA. Demonstrating a Direct-Injection Constant-Volume Combustion Chamber As a Validation Tool for Chemical Kinetic Modeling of Liquid Fuels. ASME 2018 Internal Combustion Engine Division Fall Technical Conference, San Diego, California, Nov. 4–7, 2018. DOI:10.1115/ICE-F2018-9729.

[30] M. Tao, P. Zhao, J.P. Szybist, P. Lynch, H. Ge Insights into engine autoignition: combining engine thermodynamic trajectory and fuel ignition delay iso-contour. Combust Flame 2019;200:207–218. doi:10.1016/j.combustflame.2018.11.025.

[31] D.M. Cameron Autoignition studies of gasoline surrogate fuels in the advanced fuel ignition delay analyzer Graduate Theses & Dissertations. University of Colorado Boulder Mechanical Engineering; 2017. p. 150.

[32] Goodwin DG, Speth RL, Moffat HK, Weber BW. Cantera: An object-oriented software toolkit for chemical kinetics, thermodynamics, and transport processes, Version 2.4.0, https://www.cantera.org; 2018.

[33] Richards KJ, Senecal PK, Pomraning E. CONVERGE 2.4, Convergent Science, https://convergecfd.com; 2018.

[34] Reitz R D, Diwakar R. Structure of High-Pressure Fuel Sprays. SAE Technical Paper 1987. DOI:10.4271/870598.

[35] R.D. Reitz Modeling atomization processes in high-pressure vaporizing sprays. Atomisation and Spray Technology 1987;3:309–337.

[36] M.A. Patterson, R.D. Reitz Modeling the effects of fuel spray characteristics on diesel engine combustion and emissions. SAE Trans 1998;107(3):27–43.

[37] D.P. Schmidt, C.J. Rutland A new droplet collision algorithm. J. Comput Phys 2000;164:62–80.

[38] Frossling N. Evaporation, heat transfer, and velocity distribution in two-dimensional and rotationally symmetrical laminar boundary-layer flow. NACA-TM-1432, 1958.

[39] Liu AB, Mather DK, Reitz RD. Modeling the Effects of Drop Drag and Breakup on Fuel Sprays. SAE Technical Paper 1993. DOI:10.4271/930072.

[40] Pomraning E, Richards K, Senecal P. Modeling Turbulent Combustion Using a RANS Model, Detailed Chemistry, and Adaptive Mesh Refinement. SAE Technical Paper 2014. DOI:10.4271/2014-01-1116.

[41] Senecal P, Pomraning E, Richards K, Briggs T, Choi CY, McDavid RM, Patterson MA. Multi-Dimensional Modeling of Direct-Injection Diesel Spray Liquid Length and Flame Lift-off Length using CFD and Parallel Detailed Chemistry. SAE Technical Paper 2003. DOI:10.4271/2003-01-1043.

[42] Lu T. Personal communication, 2018.

[43] Mehl M, Zhang K, Wagnon S W, Kukkadapu G, Westbrook C K, Pitz W J, et al. A comprehensive detailed kinetic mechanism for the simulation of transportation fuels. 10th U.S. National Combustion Meeting, College Park, MD, April 23–26, 2017.

[44] Kolodziej C, Kodavasal J, Ciatti S, Som S, Shidore N, Delhom J. Achieving Stable Engine Operation of Gasoline Compression Ignition Using 87 AKI Gasoline Down to Idle. SAE Technical Paper 2015. DOI:10.4271/2015-01-0832.

[45] R. McCormick, G. Fioroni, L. Fouts, E. Christensen, J. Yanowitz, E. Polikarpov, et al Selection criteria and screening of potential biomass-derived streams as fuel blendstocks for advanced spark-ignition engines. SAE Int J Fuels Lubr 2017;10(2):442–460. doi:10.4271/2017-01-0868.

[46] H.J. Curran, P. Gaffuri, W.J. Pitz, C.K. Westbrook A comprehensive modeling study of n-heptane oxidation. Combust Flame 1998;114(1–2):149–177. doi:10.1016/S0010-2180(97)00282-4.

[47] B. Higgins, D. Siebers, A. Aradi Diesel-spray ignition and premixed-burn behavior. SAE Transactions 2000;109:961–984.